



Published in final edited form as:

Bioconjug Chem. 2008 January ; 19(1): 39–49.

Conjugated Platinum(IV)-Peptide Complexes for Targeting Angiogenic Tumor Vasculature

Sumitra Mukhopadhyay^{†,¶}, Carmen M. Barnés^{‡,¶,*}, Ariel Haskel[†], Sarah M. Short[‡], Katie R. Barnes[†], and Stephen J. Lippard^{†,*}

[†] Department of Chemistry, Massachusetts Institute of Technology, Cambridge, Massachusetts 02139

[‡] Vascular Biology Program, Children's Hospital and Harvard Medical School, Boston, Massachusetts 02115

Abstract

The integrins $\alpha_v\beta_3$ and $\alpha_v\beta_5$ and the membrane-spanning surface protein aminopeptidase-N (APN) are highly expressed in tumor-induced angiogenesis, making them attractive targets for therapeutic intervention. Both integrins and APN recognize a broad range of peptides containing RGD (Arg-Gly-Asp) and NGR (Asn-Gly-Arg) motifs, respectively. Here, we describe the design, synthesis, and characterization of a series of mono- and difunctionalized platinum(IV) complexes in which a conjugated peptide motif, containing either RGD, CRGDC, (RGDfK)_c or NGR, is appended as a 'tumor-homing device' to target tumor endothelial cells selectively over healthy cells. Platinum(IV)-peptide complexes with non-specific amino acids or peptide moieties were prepared as controls. Concentration-response curves of these compounds were evaluated against primary proliferating endothelial cells and tumor cell lines and compared to those of cisplatin, a well-described platinum-based chemotherapeutic agent. The Pt(IV)-RGD conjugates were highly and specifically cytotoxic to $\alpha_v\beta_3$ and $\alpha_v\beta_5$ containing cell lines, approaching the activity of cisplatin. The Pt(IV)-NGR complexes were less active than Pt(IV)-RGD-containing compounds but more active than non-specific Pt-peptide controls. Integrin $\alpha_v\beta_3$ mediated, at least in part, the anti-proliferative effect of an Pt(IV)-RGD conjugate, as demonstrated by a decreased inhibitory response when endothelial cells were either (1) incubated with an excess of $\alpha_v\beta_3$ / $\alpha_v\beta_3$ -specific RGD pentapeptides, or (2) transfected with RNAi for β_3 , but not β_1 , integrins. These results suggest a rational approach to improved chemotherapy with Pt(IV)-peptide conjugates by selective drug delivery to the tumor compartment.

Introduction

Cisplatin, *cis*-diamminedichloroplatinum(II), is standard chemotherapy for testicular, ovarian, cervical, head, neck, esophageal, and non-small cell lung cancer (1-6). Cisplatin displays limited activity toward the more common colon and breast cancers, however, and toxic side effects are associated with its intake (1). A key objective of our current research program is to synthesize novel Pt-based drugs with equal potency but reduced toxicity derived from their ability to target tumor tissue. Targeted platinum therapy has the potential to increase the net amount of platinum that reaches the tumor environment, thereby decreasing the amount of platinum required and consequently reducing side effects on healthy, non-cancerous tissues.

Tumor cell survival, growth, and metastasis are driven by angiogenesis, the process by which new blood vessels are formed (7-9). Tumor blood vessels are permeable and morphologically distinct from normal blood vessels. Because the tumor endothelial cell can be selectively

*To whom correspondence should be addressed. Email: carmen.barnes@childrens.harvard.edu, lippard@mit.edu.

¶These authors contributed equally to the work

recognized, it has become a major target for treating cancer (10). Among the cell surface proteins upregulated in endothelial cells and on certain tumor cells during tumor growth and metastasis are the $\alpha_v\beta_3$ and $\alpha_v\beta_5$ integrins (11-13) and aminopeptidase-N (APN or CD13) (14), which are absent or barely detectable in resting endothelial cells. Integrins are transmembrane-spanning receptors that participate in cell-cell and cell-matrix interactions in all normal and malignant cell types (15,16). The integrin $\alpha_v\beta_3$ plays a critical role in the adhesion and migration of endothelial cells to extracellular matrix components. Integrins $\alpha_v\beta_3$ and $\alpha_v\beta_5$ and APN recognize the peptide motifs RGD (Arg-Gly-Asp) (17,18) and NGR (Asn-Gly-Arg) (14), respectively, with high affinity. The $\alpha_v\beta_3$ integrin can also bind NGR but with lower affinity (19). RGD- and NGR-containing peptide motifs and peptidomimetics specifically target the tumor vasculature (10,14,20) and have been evaluated as antagonists of $\alpha_v\beta_3$ and APN. RGD-containing peptides compete in the binding of ECM proteins to cell surface $\alpha_v\beta_3$ and $\alpha_v\beta_5$, preventing cellular adhesion to the extracellular matrix, thwarting cell metastasis, and inducing apoptosis (21,22). Linear and cyclic RGD peptide motifs have been employed as delivery agents for small molecular weight drugs, peptides, and proteins to the tumor endothelial cells, as recently reviewed (23).

On the basis of these findings, we have developed a strategy to prepare new platinum(IV) anticancer drug candidates in which the conjugated peptide motif, containing either RGD or NGR, would serve as a 'tumor-targeting device' and selectively kill angiogenic tumor endothelial cells. Here we describe the design, synthesis, and characterization of the first such conjugates, mono- and difunctionalized Pt(IV)-peptide complexes. As previously reported for platinum(IV) analogues containing a tethered steroid hormone moiety, reduction in the cell releases the axially appended ligand to unmask cisplatin (24).

As targeting moieties, we have used the RGD and NGR linear tripeptides; an RGD-containing disulfide-bridged cyclic pentapeptide, (CRGDC)_c; and the cyclic pentapeptide, (RGDfK)_c. CRGDC and (RGDfK)_c were chosen because cyclic peptides target angiogenic endothelial cells more efficiently compared to their linear counterparts (12,21,25,26). The two cysteine residues in CRGDC form a disulfide bond which gives the RGD portion a constrained bent structure that facilitates specific recognition by the integrins on the cell surface (20,21,25,26). (RGDfK)_c is an antiangiogenic peptide derived from the $\alpha_v\beta_3$ and $\alpha_v\beta_5$ inhibitor (RGDfV)_c. (RGDfK)_c preserves the biological activity of its parent compound (27) but can be readily attached to different moieties through the lysine ϵ -amino group without losing its selectivity properties (28). In addition, several other Pt(IV) compounds linked to a nonspecific amino acid or a tripeptide have been prepared as controls.

All peptides or amino acid residues were attached by means of an amide bond to the terminal carboxylate group of the axially coordinated succinato ligands in *cis, cis, trans*-diamminedichlorodisuccinatoplatinum(IV) complex, *cis, cis, trans*-[Pt(NH₃)₂Cl₂(succinate)₂] (**1**) (24). Numerical designations and abbreviations of these complexes and their charges at pH 7 are given in Chart 1. Concentration-response curves of these Pt(IV)-peptide complexes along with that of cisplatin and **1** were assessed against different primary endothelial cells and tumor cell lines, which include bovine capillary endothelial (BCE) cells, human umbilical vein endothelial cells (HUVEC), human dermal microvascular endothelial cells (HMVEC), human glioblastoma (U87), human pancreatic carcinoma (ASPC1), human uterine sarcoma (MES-SA), and human cervical carcinoma (HeLa) cells. We found that both endothelial cells and the tumor lines tested were positive either for both $\alpha_v\beta_3$ and $\alpha_v\beta_5$ or for $\alpha_v\beta_5$ integrins. The activity profiles of all the platinum complexes against these cells are described herein.

Experimental Procedures (29)

Materials

Potassium tetrachloroplatinate(II) was a gift from Englehard. Cisplatin, *cis, cis, trans*-diamminedichlorodihydroxyplatinum(IV), and *cis, cis, trans*-diamminedichlorodisuccinatoplatinum(IV) were synthesized according to literature procedures (24,30,31). (RGDfK)c was prepared as reported (32,33). Chemicals and solvents were of reagent grade quality and used as received from commercial suppliers.

Instrumentation and Analytical Measurements

An Advanced ChemTech automated instrument (Model ACT 348 Ω) was used for peptide synthesis. HPLC purifications using C18 analytical (VYDAC, 4 mm \times 250 mm) and C18 semi-preparative (VYDAC, 40 mm \times 250 mm) columns were performed with Waters instrumentation comprising a 600S system-controller coupled with an absorption detector (Waters 2487) and pump (Waters 616). Purifications with a C18 preparative (VYDAC, 100 mm \times 250 mm) column used a Waters 600E system-controller coupled with an absorption detector (Waters 486) and pump (Waters 600). LC-MS analyses were performed on an Agilent 1100 series instrument using a ZORBAX extended SB-C18 column of dimensions 4.6 mm \times 150 mm and a ZORBAX 80A extended C18 column of dimensions 2.1 mm \times 100 mm. High-resolution mass spectral analyses were performed at the MIT Department of Chemistry Instrument Facility (DCIF).

Synthesis of Peptides and Platinum Complexes

RGD, NGR, AGR, (CRGDC)c—The linear peptides were prepared by using the standard Fmoc protocol on an automated peptide synthesizer. The rink amide resin with a loading capacity of 0.61 mmol/g was used as the solid support. In a typical 16-well synthesis, a total of 1.2 g (0.74 mmol) of the resin and a ten-fold excess of each amino acid (7.36 mmol) in 24 mL of *N*-methyl-2-pyrrolidinone (NMP) solution were used in the presence of 1,3-diisopropylcarbodiimide (DIC), acetic anhydride, 1-hydroxybenzotriazole (HOBT), and diisopropylethylamine (DIPEA) (0.5 M solution of each in DMF). Fmoc-Asn(Trt)-OH, Fmoc-Asp(OtBu)-OH, Fmoc-Arg(Pbf)-OH, and Fmoc-Cys(Trt)-OH provided sources of Asn, Asp, Arg, and Cys, respectively. The Fmoc protecting group was removed with a 20% piperidine solution in DMF. After the synthesis, the peptides were cleaved from the resin with a solution of 95% TFA, 2.5% triisopropylsilane (TIPS), and 2.5% water to obtain amide functionalization at the C-terminus. The resulting peptides were precipitated by cold ether. The aqueous solution of linear CRGDC was air oxidized overnight to form the S–S bridged (CRGDC)c. The purification of these peptides was carried out by reverse-phase HPLC by using a C18 preparative column (VYDAC, 100 mm \times 250 mm) in greater than 90% yield. Their purity was verified by LC-MS and mass spectrometry. ESI-MS: for RGD: Calcd [M+H]⁺ 346.36 amu; Found 346.3 amu; for NGR: Calcd [M+H]⁺ 345.38 amu, Found 345.51 amu; for AGR: Calcd [M+H]⁺ 302.35 amu, Found 302.29 amu; and for (CRGDC)c: Calcd [M+H]⁺ 550.2 amu, Found 550.4 amu.

RGD-Conjugated Diamminedichloroplatinum(IV) Complexes (2a and 2b)—To a solution of **1** (0.025 g, 0.043 mmol) in 200 μ L of water was added a 100 μ L solution of EDC (0.082 g, 0.43 mmol), followed by a 100 μ L solution of NHS (0.050 g, 0.43 mmol) with vigorous stirring. This solution was then added to an aqueous solution (200 μ L) of RGD tripeptide (0.075 g, 0.22 mmol) in a dropwise manner. The reaction mixture was stirred for ~24 h in dark. The products were purified by reverse-phase HPLC (C18 semi-preparative column, 40 mm \times 250 mm, linear gradient from 100% H₂O to 15% acetonitrile over 30 min). The mono-(**2a**) and diconjugated (**2b**) products were collected separately and lyophilized to yield ~4.3 mg of **2a** (11.6% with respect to the starting complex, **1**) and ~2.4 mg of **2b** (5%

with respect to **1**). The purity of these complexes was confirmed by LC-MS and mass spectrometry. ESI-MS: for **2a**, Calcd $[M+H]^+$ 861.1665 amu, Found 861.1646; for **2b**, Calcd $[M+H]^+$ 1188.332 amu, Found 1188.3235 amu; and Calcd $[(M+2H)/2]^{2+}$ 594.6699 amu, Found 594.6680 amu.

NGR-Conjugated Diamminedichloroplatinum(IV) Complexes (3a and 3b)—These complexes were prepared and purified following the same procedure described above for **2a** and **2b** except that the linear NGR tripeptide was used instead of RGD, and a shorter linear gradient was used in the HPLC purification (25 min). The mono- (**3a**) and diconjugated (**3b**) products were collected separately and lyophilized to afford 14% of **3a** and 8% of **3b**. The purity of these complexes was confirmed by LC-MS and mass spectrometry. ESI-MS: for **3a**, Calcd $[M+H]^+$ 860.1825 amu, Found 860.1618; for **3b**, Calcd $[M+H]^+$ 1186.3639 amu, Found 1186.3735 amu; and Calcd $[(M+2H)/2]^{2+}$ 593.6859 amu, Found 593.6715 amu.

AGR-Conjugated Diamminedichloroplatinum(IV) Complexes (4a and 4b)—These complexes were prepared and purified by following the same procedure as **2a** and **2b** but with the linear AGR tripeptide instead of RGD. The mono- (**4a**) and diconjugated (**4b**) products were collected separately and lyophilized to afford 16% of **4a** and 7% of **4b**. The purity of these complexes was confirmed by LC-MS and mass spectrometry. ESI-MS: for **4a**, Calcd $[M+H]^+$ 817.1766 amu, Found 817.1735 amu; for **4b**, Calcd $[M+H]^+$ 1100.3523 amu, Found 1100.372 amu; and Calcd $[(M+2H)/2]^{2+}$ 550.68 amu, Found 550.50 amu.

Glycinamide-Conjugated Diamminedichloroplatinum(IV) Complexes (5a and 5b)—These complexes were prepared by following a procedure similar to that for the other platinum(IV)-peptide conjugates except that glycinamide was used instead of a tripeptide. The complexes were purified as described for **3a** and **3b**. The mono (**5a**) and diconjugated (**5b**) products were collected separately and lyophilized to afford ~50% of **5a** and ~44% of **5b**. The purity of these complexes was confirmed by LC-MS and mass spectroscopy. ESI-MS: for **5a**, Calcd $[M+H]^+$ 590.0384 amu, Found 590.0389 amu; for **5b**, Calcd $[M+H]^+$ 646.0759 amu, Found 646.0757 amu.

(CRGDC)c-Conjugated Diamminedichloroplatinum(IV) Complex (6)—This complex was prepared by following the same procedure as described above for the Pt(IV)-RGD complexes using (CRGDC)c peptide. A white precipitate, observed in the reaction mixture upon stirring overnight, was discarded by filtration. In this case, however, the diconjugated complex was not detected by LC-MS or HPLC. The monoconjugated product, **6**, was purified by reverse-phase HPLC as described above for **2a** and lyophilized to afford the product in ~10% yield. The purity of this complex was confirmed by LC-MS and mass spectrometry. ESI-MS: for **6**, Calcd $[M+H]^+$ 1066.17 amu, Found 1066.2 amu.

(RGDfK)c-Conjugated Diamminedichloroplatinum(IV) Complexes (7a and 7b)—These complexes were prepared by following a procedure similar to that for the other platinum(IV)-peptide conjugates except that the cyclic pentapeptide, (RGDfK)c, was used instead of a tripeptide and the lysine ϵ -amino group of (RGDfK)c was activated with DIPEA prior to reaction with **1**. The products were purified by reverse-phase HPLC as described above for **3a** and **3b**. The mono- (**7a**) and diconjugated (**7b**) products were collected separately and lyophilized to afford ~12% of **7a** and ~8% of **7b**. The purity of these complexes was confirmed by LC-MS and mass spectroscopy. ESI-MS: for **7a** Calcd $[M+H]^+$ 1120.30 amu, Found 1120.20 amu; for **7b** Calcd $[M+H]^+$ 1705.61 amu, Found 1705.3 amu; and Calcd $[(M+2H)/2]^{2+}$ 853.81 amu, Found 853.80 amu.

Cell Culture—Endothelial and tumor cells were all grown at 37 °C under a 5% CO₂ atmosphere, except for bovine capillary endothelial (BCE) cells, which were grown at 10% CO₂. BCEs were isolated from bovine adrenal cortex and cultured in pre-gelatinized tissue culture plates in Dulbecco's modified Eagle's medium (DMEM; Invitrogen/GIBCO) containing 10% bovine calf serum (Hyclone Laboratories, Logan, UT) and 3 ng/mL basic fibroblast growth factor (bFGF), and 1% GPS, as previously described (34). Human dermal microvascular endothelial cells (HMVEC-d; Lonza Inc. and Cascade Biologics, Portland, OR, USA) and human umbilical vein endothelial cells (HUVEC; Lonza Inc.) were maintained according to supplier's directions. HMVEC-d were cultured in microvascular endothelial growth medium (EGM-MV; Cambrex Bio Science); human umbilical vein endothelial cells (HUVEC; Cambrex Bio Science) were cultured in endothelial growth medium-2 (EGM-2; Cambrex Bio Science). All endothelial cells were plated on pre-gelatinized tissue culture plates (1.5% gelatin in PBS). Human glioblastoma cell line U87, purchased from the American Type Culture Collection (ATCC, Rockville, MD, USA), and HeLa cells were grown in DMEM supplemented with 10% heat-inactivated (56 °C for 40 min) fetal calf serum (hi-FCS) (Invitrogen/GIBCO, Grand Island, NY), 2 mM L-glutamine, and 1% penicillin-streptomycin (GPS, glutamine/penicillin/streptomycin; Invitrogen/GIBCO). Human uterine sarcoma MES-SA cells (ATCC) were cultured in modified McCoy's 5a medium (ATCC) supplemented with 10% hi-FCS and 1% GPS. Human pancreatic adenocarcinoma cell line ASPC-1 (ATCC) was cultured in RPMI 1640 (ATCC) containing 10% hi-FBS and 1% GPS.

Concentration-Response Curves of Platinum Complexes—BCE cells were plated at 7.5×10^3 cells per well in DMEM containing 10% bovine calf serum. After overnight incubation at 37 °C (in 10% CO₂), the media was replaced with DMEM containing 5% BCS, 2.0 ng/ml, and various concentrations of the Pt-compound (stock solutions prepared in PBS) to a final concentration range of 10 nM to 1 mM. Wells with and without bFGF in the absence of platinum complex were kept as positive and negative controls, respectively. All concentrations were tested in triplicate. After 72 h, viable cells were trypsinized (Trypsin-EDTA; Invitrogen/GIBCO BRL), resuspended in isotonic diluent (Fisher Scientific, Pittsburgh, PA), and counted using a particle counter. Data were analyzed as described below.

HMVEC-d (passages 2-5) were seeded at 7.5×10^3 cells per well in pre-gelatinized 48-well plates in endothelial basal medium (EBM-2; Cambrex Bio Science) supplemented with 5% FBS and incubated at 37 °C (in 5% CO₂). After 24 h, the media was replaced with microvascular endothelial growth medium (EGM-MV) and the Pt-compound dissolved in PBS (10% volume) or PBS alone (positive control). For the negative control, the media was replaced with EBM-2 supplemented with 5% FBS instead. Cells were incubated for 72 h, trypsinized, and counted on a particle counter. HUVEC were performed as described for HMVEC-d with the following changes. Cells were plated in EBM-2 supplemented with 2% FBS, challenged with EGM-2, and EBM-2 containing 2% FBS was used as a negative control.

To investigate the effect of Pt(IV) complexes in tumor lines, tumor cells were seeded at a density of 5.0×10^3 cells per well. For plating and challenging, the corresponding cultivation media supplemented with 5% hi-FBS and 1% GPS were used (DMEM in the case of U87 and HeLa cells; modified McCoy's 5a medium was employed in the case of MES-SA and MES-SA/Dx; RPMI-1640 for ASPC-1). After 24 h, the media was replaced with fresh media containing 5% FCS and the Pt-compound dissolved in PBS (10% volume). Cells were incubated for 72 h, trypsinized, counted on a particle counter, and analyzed as described below.

Analysis of Concentration-Response Curves and Determination of IC₅₀ Values—Cell numbers determined from the concentration-response curves were converted to percent cell number. For each cell line and each compound tested, the data for all independent experiments (2-9) were combined and analyzed by non-linear regression to a hyperbolic decay

equation. The data were fitted by using SigmaPlot 8.0 to a 2-parameter hyperbolic decay model $y = a \times b / (b + x)$, where $y = \% \text{ cell number}$ and $x = \text{concentration of platinum compound}$. A 3-parameter hyperbolic decay model ($y = y_0 + a \times b / (b + x)$), tested both in the absence and presence of constraints ($a = 95, y_0 = 5$), yielded larger P-values, and was therefore not used. The IC_{50} values were determined based on the fitted data, and standard error and P values were derived from the b parameter.

Competition Studies in BCE with Free Peptides—BCE cells were plated as described for the concentration-dependent curves. After 24h, the medium was replaced with DMEM containing 5% BCS, 2.0 ng/ml basic fibroblast growth factor, with or without **2a** (2 μ M) and with or without various concentrations of RGD peptides (0.1-1 mM). The effects of the RGD tripeptide, the cyclic pentapeptide (CRGDC)c, and the cyclic pentapeptide (RGDfK)c, in **2a**-treated cell proliferation were assessed. Wells with and without bFGF in the absence of platinum complex were kept as positive and negative controls, respectively. All concentrations were tested in triplicate. After 72 h, viable cells were trypsinized and counted using a particle counter. Data were analyzed as described above.

siRNA Transfection—The β_1 , β_3 , and α_v integrins and control siRNAs were purchased as four oligonucleotide SmartPools (Dharmacon Research, Inc.), containing an approximate 50% guanidine-cytosine content (Dharmacon Research, Inc.). Subconfluent HMVEC-d were washed with HBSS and transfected with 10nM siRNAs using SiLentFect (Biorad) following manufacturer's protocol. The medium was changed after a 4-h transfection period. Cells were trypsinized 24 h post-transfection and plated onto gelatin-coated 48-well plates at a density of 7500 cells/well, in EBM-2 supplemented with 5% FBS. After overnight incubation at 37 °C, cells were challenged with either **2a** or cisplatin. Cells were counted after 72 hours, and results were analyzed as described above.

Western Analysis—Downregulation of protein expression following RNAi interference was confirmed by Western analysis of cell lysates harvested 120 hours post-transfection, and at the same time proliferation plates were counted. Lysate preparation and Western analysis were performed as described previously (35). mAbs against integrin subunits included: anti- β_1 (clone B3B11, Chemicon International), anti- β_3 (R&D Systems), anti- α_v (Chemicon). mAb against α -actin (Abcam) was used as control for equal protein loading. Immunoreactivity was detected on Hyperfilm using ECL (Amersham Biosciences). Films were scanned and band intensities were quantitated with Image J 1.37 software. Band intensities were normalized to actin and shown as percent protein levels.

Fluorescence-Activated Cell Sorting—The expression of integrins $\alpha_v\beta_3$ and $\alpha_v\beta_5$ was detected by immunofluorescence in unfixed cells. Cells were briefly trypsinized, washed in PBS containing 2% FBS, and incubated on ice for 1 hr with Cy5-conjugated anti-human $\alpha_v\beta_3$ (MAB1976S) or $\alpha_v\beta_5$ (MAB1961S) monoclonal antibodies in PBS containing 2% FBS (10 μ g/ml; Chemicon, Temecula, CA). Unlabeled cells were used as negative controls. BCE and HMVEC cells were analyzed for APN expression using mouse anti-human CD13 IgG (10 μ g/ml; BD Biosciences Pharmingen, San Jose, CA). Mouse IgG was used as negative control. After incubation on ice for 1 hr, the cells were washed 3 times in PBS containing 2% FBS, incubated with FITC-labeled horse anti-mouse IgG (1:100) (Vector Laboratories, Burlingame, CA) for an additional hour, and then washed again. Cells were analyzed on a fluorescence-activated cell sorting (FACS) VantageSE flow cytometer using the Cell Quest software (Beckton Dickinson, San Jose, CA). For each cell type, the fluorescence emitted by negative control cells was used to set a threshold gate. FITC or Cy5-labeled cells emitting higher fluorescence than the threshold value were considered positive and were used to determine the

percentage of positively-labeled cells. Each experiment was performed twice. FACS images were overlaid in Adobe Photoshop 7.0.

Results and Discussion

Synthesis and Characterization of Pt(IV)-Peptide Conjugates

Cisplatin and other platinum(II) drugs are generally administered to patients intravenously, whereas platinum(IV) agents can be taken orally because of their greater stability in the gastrointestinal (G. I.) tract (31,36). One such compound, *cis,trans,cis*-amine(cyclohexylamine) diacetatodichloroplatinum(IV), or satraplatin, is currently in a Phase III clinical trial for hormone-refractory prostate cancer (37). Whereas the half-life of satraplatin in tissue culture medium and human plasma is long (22 h and 5.3 h, respectively), the Pt(IV) compound undergoes rapid biotransformation in blood to a Pt(II) species, with a half-life of only 6.3 minutes (38). The Pt(II) metabolite of satraplatin, *cis*-amine(cyclohexylamine) dichloroplatinum(II), forms DNA cross-links that are structurally very similar to those of cisplatin (39).

A targeted Pt(IV) complex requires a sufficiently long half-life to reach the tumor environment. Because the average cardiac output in an adult resting human is 5 liters per minute, and the average total circulating volume in an adult male is 5 liters, it takes approximately 1 minute for the blood to circulate once through the body. Based on the satraplatin half-life in blood, we estimate that an intravenous administration of a targeted Pt(IV) compound should have sufficient time to reach the tumor site before its conversion to Pt(II).

By exploiting integrin- and APN-specific peptide recognition as the guiding strategy, we have designed new Pt(IV) anticancer drug candidates for targeting angiogenic tumor endothelial cells and tumor cells expressing such integrins. The RGD and NGR containing tri- and pentapeptide sequences in these molecules are tethered as axial ligands to the Pt(IV) center. Following selective binding to the tumor cell surfaces, these Pt(IV) species have the potential to enter the cells where they will be readily reduced by glutathione or other intracellular reductants to afford cisplatin (40-42). If successful, the level of toxicity of these complexes towards normal cells should be greatly diminished.

cis,trans,cis-Diamminedisuccinatodichloroplatinum(IV), *cis-cis-trans*-[Pt-(NH₃)₂(succinate)₂Cl₂] (**1**), was employed as the precursor in the synthesis of all Pt-peptide conjugates. Compound **1**, prepared as reported elsewhere (24), is suitable for additional derivatization at its axial positions by appropriate coupling with the terminal carboxylate groups of the succinato moieties. A similar strategy was employed successfully in our laboratory to obtain a series of estrogen-tethered platinum(IV) compounds, which are capable of inducing the over-expression of HMGB1 (high mobility group binding protein 1) in MCF-7 cells and thus sensitizing them to the conjugates (24).

Three different tripeptide sequences, RGD, NGR, and AGR, and the disulfide-bridged pentapeptide, (CRGDC)_c, were prepared by solid-phase synthesis. The -SH groups of cysteine residues in linear CRGDC peptide were oxidized in air to form intrapeptide S-S bridged (CRGDC)_c. The peptides were purified by reverse-phase HPLC on a C18 column and characterized by LC-MS, MALDI, and ESI-MS. The cyclopentapeptide, (RGDfK)_c, was prepared by following the literature procedure (32,33).

Five monofunctionalized Pt^{IV}(NH₃)₂Cl₂-peptide conjugates, denoted as Pt-RGD-mono (**2a**), Pt-NGR-mono (**3a**), Pt-AGR-mono (**4a**), Pt-(CRGDC)_c-mono (**6**), and Pt-(RGDfK)_c-mono (**7a**), and four difunctionalized analogues designated Pt-RGD-bis (**2b**), Pt-NGR-bis (**3b**), Pt-AGR-bis (**4b**), and Pt-(RGDfK)_c-bis (**7b**), were synthesized (Scheme 1). These complexes

form upon treatment of **1** with peptide molecules in aqueous solution in the presence of 1-[3-(dimethylamino)propyl]-3-ethylcarbodiimide (EDC) and N-hydroxysuccinimide (NHS) as activator and coupling reagents. In the case of (RGDFK)_c, the ε-amino group of the lysine side chain was activated with a base, DIPEA, before it was allowed to react with **1**. Except for the (CRGDC)_c peptide, these reactions afforded both mono- and diconjugated Pt-peptide species, which were separated and purified by reverse-phase HPLC. An HPLC chromatogram for the purification of linear RGD conjugated Pt(IV) complexes, **2a** and **2b**, is shown in Figure S1 (Supporting Information). For the (CRGDC)_c peptide, no difunctionalized complex was detected in the reaction mixture. In addition to the aforementioned complexes, a single amino acid residue, glycine, was tethered to the succinato group(s) in a similar fashion to obtain mono and difunctionalized Pt(IV) conjugates, **5a** and **5b**. These complexes were characterized by LC-MS and high-resolution ESI-MS. The experimental mass-spectral data are in excellent agreement with the calculated values and display the proper isotopic mass distribution patterns (see Figure S2, Supporting Information, for representative mass spectra). Lower yields were obtained for the platinum-peptide conjugates by comparison to the glycine-platinum conjugates. The decreased yield is most likely the consequence of steric effects generated by the longer amino acid side chains of tri- and pentapeptides. In contrast, glycine is a single amino acid containing hydrogen as a side chain; therefore, the coupling reaction is facilitated.

Concentration-Response Curves of the Pt(IV)-Peptide Conjugates on Proliferating Cells

In vitro activity studies of the monofunctionalized (**2a-5a**, **6** and **7a**) and difunctionalized (**2b-5b** and **7b**) platinum(IV) complexes, as well as cisplatin and **1**, were performed on proliferating endothelial and tumor cells that express APN and/or the integrins $\alpha_v\beta_3/\alpha_v\beta_5$, discussed above. Cisplatin was used as positive control; compounds **4a**, **4b**, **5a**, and **5b**, and complex **1** were investigated as negative controls. We used primary cultures of endothelial cells, including bovine capillary endothelial (BCE) cells, human microvascular endothelial cells (HMVEC), and human umbilical vein endothelial cells (HUVEC). The tumor cell lines glioblastoma (U87), pancreatic carcinoma (ASPC1), uterine sarcoma (MES-SA and MES-SA/Dx-5), and cervical (HeLa) were also tested based on their expression of at least one of the two $\alpha_v\beta_3$ or $\alpha_v\beta_5$ integrins (43-47), which we determined by fluorescence-activated cell sorting (Figure S4). The expression of aminopeptidase-N (CD13) was also confirmed in BCE and HMVEC cells. As shown in Table 1 and supplementary figure S4, only endothelial cells and the tumor lines U87 and ASPC1 expressed $\alpha_v\beta_3$; all cells expressed $\alpha_v\beta_5$.

Cell growth was evaluated in sub-confluent, serum- and growth factor-stimulated endothelial cells or serum-stimulated tumor cells in the presence or absence of Pt compounds. BCE cells were stimulated with basic fibroblast growth factor (bFGF); HMVEC and HUVEC were stimulated with endothelial growth media containing bFGF, insulin-like growth factor 1 (IGF-1), hepatocyte growth factor (HGF), and vascular endothelial growth factor (VEGF). The activities of the platinum complexes were determined after 72 h by comparing the number of viable cells as a function of platinum concentration in treated versus untreated cells. Short pre-incubation times (2 h or 6 h) of cisplatin and **1** with BCE and HMVEC cells afforded limited decrease in cell viability, indicating the rates of internalization of platinum complexes to be relatively slow. The activities of these complexes were independent of serum concentration, tested at 5 and 10% (data not shown).

Concentration-response curves of the platinum-peptide complexes in all the cells were compared to those with cisplatin and **1**. To ensure unbiased data, two additional independent double-blinded experiments with all the complexes were performed in BCE cells, with reproducible results.

Inhibition of BCE and HMVEC Proliferation by Pt(IV) Conjugates

The IC_{50} values of these complexes, defined as the concentration at which 50% of the cells are viable, were determined for BCE and HMVEC and are summarized in Table 2.

The concentration-response curves of the monoconjugated and diconjugated platinum(IV) complexes, together with that of cisplatin and **1**, toward the BCE cells are plotted in Figures 1A and 1B, respectively. Among all these complexes, cisplatin was most efficient at inhibiting cell growth ($IC_{50} \approx 1.1 \mu\text{M}$). All Pt(IV) compounds containing conjugated targeting moieties were significantly more inhibitory than **1**, with difunctionalized and monofunctionalized compounds being equally effective. Targeted complexes **2a**, **2b**, containing the linear RGD tripeptide, and **7a**, **7b**, containing the (RGDfK)_c pentapeptide, were the most active ($IC_{50} \approx 2.1 - 3.4 \mu\text{M}$), followed by **3a** and **3b** consisting of NGR tripeptide. In contrast, all platinum (IV) conjugates containing non-targeting peptides or amino acid residues were equal to or less active than **1**. The monofunctionalized compounds **4a** and **5a** are comparable in activity to **1** ($IC_{50} \approx 18.5 \mu\text{M}$), whereas their difunctionalized counterparts are less active (**4b**, **5b**) ($IC_{50} \approx 29 \mu\text{M}$).

A similar inhibitory trend was observed when the complexes were tested on HMVEC (Figure 2). The Pt(IV)-RGD conjugates, mainly **6**, **7a** and **7b**, were most potent at inhibiting proliferation ($IC_{50} \approx 2.7-3.4 \mu\text{M}$) and comparable to cisplatin ($IC_{50} \approx 1.2 \mu\text{M}$), followed by **2a**, **2b** and the Pt-NGR conjugates, **3a** and **3b** ($IC_{50} \approx 4.5-5.9 \mu\text{M}$). Non-targeting platinum (IV) complexes, **1**, **4a**, **4b**, **5a** and **5b** were approximately an order of magnitude less potent ($IC_{50} \approx 33-55 \mu\text{M}$) (see Table 2).

The enhanced activity of RGD-containing Pt(IV) compounds was not caused by the targeting peptide moiety, as shown in Figure 1C. None of the free peptides, RGD, (CRGDC)_c, or (RGDfK)_c inhibited BCE growth, even at very high concentrations. In addition, non-conjugated 1:1 and 2:1 mixtures of free-RGD and **1** did not improve the concentration-response of **1** ($IC_{50} \approx 36 \mu\text{M}$) (data not shown). These results are consistent with the inhibitory properties of RGD peptides in vitro. RGD-peptides interfere with cellular adhesion and migration by antagonizing the interaction between integrins and the extracellular matrix, but do not affect cellular proliferation when administered to sub-confluent pre-adherent cells, as is the case in our study.

Competition Studies of **2** with Free RGD-Containing Peptides in BCE

To determine whether the increased inhibitory response of RGD-containing platinum compounds could be blocked with an excess of RGD-containing peptides, we performed competition studies in BCE cells using **2a** as the RGD-platinum compound, and RGD, (RGDfK)_c and (CRGDC)_c as the free peptides. As shown in Figure 3, the more constrained cyclic pentapeptides (CRGDC)_c (purple) and (RGDfK)_c (light green) could partially decrease the inhibitory effect of **2a** in BCE cells treated with 2 μM of the Pt-RGD compound, and this effect was statistically significant. In contrast, the RGD tripeptide had no effect, even at mM concentrations (light blue). By themselves, none of the free peptides affected BCE proliferation ((CRGDC)_c in gray, (RGDfK)_c in dark green, and RGD in dark blue), consistent with our previous findings (Figure 1C). The fact that the integrin-specific $\alpha_v\beta_3$ and $\alpha_v\beta_5$ ligand (RGDfK)_c could reduce the inhibitory effect of the mono-functionalized RGD-Pt(IV) compound suggests that these integrins are playing a role in the recognition of RGD-containing Pt(IV) compounds.

Concentration-Response curves in HMVEC-d lacking α_v , β_1 , and β_3 integrins

Although the RGD tripeptide can bind to eight of the 24 known integrin heterodimers of the integrin family, only three of these, $\alpha_5\beta_1$, $\alpha_v\beta_3$, and $\alpha_v\beta_5$ have been reported to be expressed

in endothelial cells (reviewed in (48)). Integrin levels $\alpha_5\beta_1$, $\alpha_v\beta_5$ and $\alpha_v\beta_3$ are increased, mobilized, or induced during angiogenesis, respectively, and they can promote apoptosis of angiogenic endothelial cells in vitro and in vivo (reviewed in (48)). To determine whether some or all of these integrins are responsible for the increased sensitivity of cells toward RGD-containing platinum compounds, we performed RNAi interference studies on HMVEC-d cells. HMVEC-d cells were transfected with β_1 , β_3 , α_v or control RNAi, and loss of the integrins was confirmed by Western analysis at the end of the experiment (120 hours post-transfection). Complete knockdown of the integrins was obtained for β_1 and β_3 but not for α_v , for which a significant decrease in protein expression was achieved (Figure 4E,F). An increase in β_3 and β_1 protein expression was observed in cells transfected with β_1 and α_v , respectively, suggesting compensation by other integrin pairs. This was not the case of β_3 -transfected cells, for which a decrease in α_v integrin was also observed.

Cells were plated 24 hours after RNAi transfection, treated with either cisplatin or **2a**, and counted 3 days after treatment. We found poor cell growth in HMVEC-d transfected with β_3 RNAi. The cell numbers in β_3 knockdown cells 72 h post-treatment were nearly identical to the number of plated cells, demonstrating the critical role of β_3 integrin in endothelial cell proliferation (See Figure 4B,D). In contrast, HMVEC-d transfected with control RNAi, α_v , and β_1 integrins proliferated and had comparable cell numbers at the end of the experiment.

Despite differences in cell growth between the integrin knockdown HMVEC cells, cisplatin treatment afforded identical concentration-response curves (Fig. 4A). In contrast, a shift in IC₅₀ was obtained with **2a** (Fig. 4C), particularly with β_3 knockdown (5 to 13 μ M), demonstrating that this integrin is involved in **2a**-mediated inhibition of cell growth (See also Table 4). Integrin β_5 could be compensating for the remaining targeting in the β_3 knockdown cells. Although, α_v RNAi transfections were intended to remove the contribution from $\alpha_v\beta_3$ and $\alpha_v\beta_5$ integrins, it was not possible to knock down α_v entirely (Figure 4 E,F), possibly due to the importance of integrin $\alpha_v\beta_3$ in endothelial cell proliferation. The low levels of α_v found in α_v -transfected HMVEC-d may be sufficient to mediate an inhibitory effect by RGD-Pt(IV). Given the differences in β_1 expression in β_1 and α_v -transfected cells (Figure 4 E,F) and their similarities in IC₅₀ values (Table 4), β_1 is most likely not involved in the inhibition of cell proliferation by **2a**.

Because the (RGDfK)c pentapeptide specifically binds to $\alpha_v\beta_3$ and $\alpha_v\beta_5$, and our results with RGD- and (RGDfK)c-Pt(IV) conjugates are comparable, recognition of the Pt(IV) complex by the cells most likely occurs, at least in part, through either the $\alpha_v\beta_3$ or $\alpha_v\beta_5$ integrin. This conclusion is supported by our RNAi knockdown studies. Incorporation of NGR-containing Pt(IV) conjugates **3a/3b** may also be mediated in part by integrin $\alpha_v\beta_3$, because this integrin binds NGR peptides, albeit with lower affinity than their RGD analogues (19). APN does not appear to be solely responsible for recognition of **3a/3b** given that the IC₅₀ values were comparable in BCE and HMVEC despite differences in their APN/CD13 expression levels (Table 1).

Inhibition of Cell Proliferation by RGD-Containing Pt(IV) Conjugates in $\alpha_v\beta_3$ Positive and $\alpha_v\beta_3$ Negative Cells

To determine whether $\alpha_v\beta_5$ could mediate delivery of the RGD-containing complexes in the absence of $\alpha_v\beta_3$, we compared the inhibition of Pt(IV) conjugates in endothelial cells or tumor lines that were positive (HUVEC, U87) and negative (MES-SA, MES-SA/DX-5, HeLa) for $\alpha_v\beta_3$. The concentration-response curves of the Pt-RGD conjugates were comparable on HUVEC, U87, ASPC1, MES-SA, and HeLa cell lines. The IC₅₀ values of these complexes and cisplatin are summarized in Table 4 (See Figure S3, Supporting Information, for U87). Because each cell type had a different sensitivity to cisplatin, the IC₅₀ ratio between **2a**/cisplatin and **7a**/cisplatin was used to compare the RGD and (RGDfK)c conjugates (see Tables 2 and

3). The best inhibitory effect was obtained in BCE, U87, ASPC1, and HeLa; because the last two cell lines are negative for $\alpha_v\beta_3$, our results suggest that $\alpha_v\beta_5$ is equally efficient at delivering Pt(IV) into the cell.

Targeting Efficiency: Linear vs. Cyclic Peptides

According to literature reports, the cyclic RGD and NGR peptides containing cysteine residues that form disulfide bonds mark angiogenic endothelial cells with more efficiency compared to their linear counterparts (20,21,25,26). It is believed that the presence of disulfide linkage in the cyclic peptides provides the RGD and NGR motifs a constrained conformational arrangement resulting in stronger interactions with the integrins expressed on the cell surfaces. In some cases, the cyclic peptides containing the RGD and NGR motifs were 10- to 200-fold more effective over the corresponding linear peptides in recognizing the receptors (21,25,26). In the present study we examined both linear RGD and cyclic CRGDC peptides to serve as the marker to transport the attached platinum complexes to the tumor cells. We also included the cyclic pentapeptide, (RGDfK)c, which is a potent inhibitor of $\alpha_v\beta_3/\alpha_v\beta_5$ (27,49).

The differential recognition of linear vs cyclic RGD peptides to integrins was indirectly confirmed in our competition studies, because both cyclic pentapeptides, (CRGDC)c and (RGDfK)c, could partially compete the inhibitory effect of **2a** in BCE cells, whereas the linear tripeptide RGD was ineffective. Although we have not yet determined the binding affinities of the linear RGD-containing Pt(IV) compounds and the cyclic RGD containing Pt(IV) complexes, our results indicate that the linear RGD tri-peptide containing Pt(IV) complexes are equally effective in inhibiting cell proliferation and cell killing. Only for about half of the cells tested did we find that the mono and diconjugated (RGDfK)c compounds were slightly superior to the mono and bis-conjugated RGD compounds (HMVEC, U87, MES-SA). As supported by the values listed in Table 3, the IC₅₀ ratios of the monoconjugated RGD containing Pt(IV) complexes, **2a** and **7a**, with respect to cisplatin are quite comparable for a given cell type. We have also demonstrated that at least some of the anti-proliferative effect of **2a** is mediated by the $\alpha_v\beta_3/\alpha_v\beta_5$ integrins, as (1) the $\alpha_v\beta_3/\alpha_v\beta_5$ integrin-specific ligand, (RGDfK)c, and (CRGDC)c could partially compete off **2a** in BCE cells, and (2) Loss of β_3 in HMVEC decreased the IC₅₀ of **2a** but not of cisplatin. It is possible that upon conjugation to the succinate group in Pt(IV), the RGD linear tripeptide and the cyclic RGD pentapeptide targeting moieties become comparable at recognizing $\alpha_v\beta_3/\alpha_v\beta_5$ integrins. The Pt(IV) center could sterically hinder binding of the cyclic pentapeptides, decreasing their enhanced binding, or the Pt(IV) center may impose a more rigid conformation to the RGD linear targeting moiety enhancing its binding potential to the $\alpha_v\beta_3/\alpha_v\beta_5$ integrins. A high degree of targeting ability with linear RGD tripeptide attached to glycosylated porphyrins was also observed in photodynamic cancer therapy against K562 leukemia cell lines (50).

Cell Internalization of Pt-Peptide Conjugates

The platinum complexes can enter the cells selectively, through internalization by a surface marker such as $\alpha_v\beta_3$ integrin, or non-selectively, by diffusion across the cell membrane or via other transporters or carriers. Cisplatin, a small neutral molecule, enters cells by passive diffusion (4) and, to a degree not yet quantified, other transporters (51,52). Differences in the size and overall charge on the complex will affect passive diffusion of the complexes through the cell membrane, with smaller, planar, and neutral complexes being more readily incorporated than large, non-planar, and charged ones. Some of our platinum-peptide complexes are neutral at pH 7 in aqueous solution, whereas a few of the complexes are positively charged and several of them are negative (Chart 1). All of the Pt(IV) complexes have an octahedral geometry which, together with their variable overall charges, makes it unlikely that they would be internalized by passive diffusion. Except for cisplatin, the non-targeted Pt-complexes should therefore enter cells by selective uptake. The toxicity profiles of the

negatively charged mono-glycinamide-tethered complex (**5a**), the neutral mono-AGR (**4a**) and bis-glycinamide complexes (**5b**) and the positively charged bis-AGR complexes (**4b**), are quite similar to that of **1**, which is smaller and negatively charged in aqueous solution. Although the monoconjugated RGD complexes are negatively charged, and the diconjugated complexes are neutral in water, they have very similar inhibitory effect and are significantly more potent than the non-targeted Pt(IV) complexes. No significant differences in anti-proliferative effect were observed between the targeted mono and di-conjugated complexes, suggesting that only one ligand is sufficient for cell surface recognition. These results indicate that the cellular uptake of the targeted platinum(IV) complexes is most likely mediated by internalization by surface markers, $\alpha_v\beta_3$ and $\alpha_v\beta_5$ integrins, which would account for their greater potency compared to the non-targeted analogues.

From the perspective of evaluating compounds for further study in animal models and, eventually, human cancer treatment, it would have been valuable to test them against cells that were $\alpha_v\beta_5$ negative. The cell lines that we tested were all positive for this integrin (Table 1), however. Nevertheless, the significantly improved effectiveness of the targeted RGD, NGR, and (CRGDC)c conjugates compared to the non-targeted AGR, Gly, and disuccinate precursor clearly establishes the value of targeting receptors involved in tumor vasculature as a strategy for improving the efficacy and selectivity of platinum-based drugs.

Conclusion

Targeted drug delivery is currently an active area of research in cancer therapy. It offers two major advantages over traditional chemotherapy: (1) it avoids damage to the normal tissue, and (2) it can limit drug resistance, which is a real concern for the current palette of platinum anticancer drugs. In the present investigation, several Pt(IV)-peptide conjugates were designed and synthesized for the purpose of targeted drug delivery to tumor endothelial cells and tumor cells expressing $\alpha_v\beta_3/\alpha_v\beta_5$ integrins. The tri- and pentapeptides, containing either an RGD or an NGR motif, attached by an amide linkage to the platinum(IV) center through a succinato group, serve as tumor-targeting units. The concentration-response curves of these complexes were examined against different endothelial and human cancer cells *in vitro*. RGD-tethered Pt(IV) complexes are potent inhibitors of cellular proliferation when compared to both non-targeted platinum(IV) compounds and to the unconjugated targeting RGD tri- and pentapeptide moieties. NGR conjugates were less inhibitory than RGD counterparts but were still more active than nonspecific Pt(IV)-peptide analogues, suggesting greater affinity of RGD units to the transmembrane receptors over NGR containing peptides. These results introduce the possibility of selective transport of platinum anticancer agents into tumor endothelial cells. Studies of the newly developed Pt(IV) RGD complexes *in vivo* are currently in progress.

Supplementary Material

Refer to Web version on PubMed Central for supplementary material.

Acknowledgements

This research was supported by grant CA34992 from the National Cancer Institute. CMB was supported by Postdoctoral Fellowship Grant #PF-03-111-01-CSM from the American Cancer Society and by the Eleanor and Miles Shore Faculty Career Development Award from Children's Hospital, Boston, MA. AH thanks the Pew Latin American Fellows Program in the Biomedical Sciences sponsored by the Pew Charitable Trusts. The MIT Department of Chemistry Instrument Facility is funded by the National Science Foundation (CHE-9808061, CHE-9808063, and DBI-9729592). We thank Prof. Judah Folkman and Catherine Butterfield at the Vascular Biology Program, Children's Hospital for helpful suggestions and for generously providing BCE cells used in this study. We thank Dr. Deborah Freedman, Children's Hospital, Boston, for providing the basic fibroblast growth factor, and Ryan Todd (Massachusetts Institute of Technology), and Arshiya Ahuja (Children's Hospital) for their experimental assistance.

Literature Cited

1. Wong E, Giandomenico CM. Current status of platinum-based antitumor drugs. *Chem Rev* 1999;99:2451–2466. [PubMed: 11749486]
2. Jamieson ER, Lippard SJ. Structure, recognition, and processing of cisplatin-DNA adducts. *Chem Rev* 1999;99:2467–2498. [PubMed: 11749487]
3. Trimmer EE, Essigmann JM. Cisplatin. *Essays Biochem* 1999;34:191–211. [PubMed: 10730196]
4. Cohen SM, Lippard SJ. Cisplatin: From DNA damage to cancer chemotherapy. *Prog Nucl Acid Res Mol Biol* 2001;67:93–130.
5. Barnes KR, Lippard SJ. Cisplatin and related anticancer drugs: Recent advances and insights. *Met Ions Biol Syst* 2004;42:143–177. [PubMed: 15206102]
6. Wang D, Lippard SJ. Cellular processing of platinum anticancer drugs. *Nat Rev Drug Disc* 2005;4:307–320.
7. Folkman J. Angiogenesis in cancer, vascular, rheumatoid and other disease. *Nat Med* 1995;1:27–31. [PubMed: 7584949]
8. Hanahan D, Folkman J. Patterns and emerging mechanisms of the angiogenic switch during tumorigenesis. *Cell* 1996;86:353–364. [PubMed: 8756718]
9. Kerbel R, Folkman J. Clinical translation of angiogenesis inhibitors. *Nat Rev Cancer* 2002;2:727–739. [PubMed: 12360276]
10. Ruoslahti E. RGD and other recognition sequences for integrins. *Annu Rev Cell Dev Biol* 1996;12:697–715. [PubMed: 8970741]
11. Brooks PC, Clark RAF, Cheresh DA. Requirement of vascular integrin $\alpha_v\beta_3$ for angiogenesis. *Science* 1994;264:569–571. [PubMed: 7512751]
12. Friedlander M, Brooks PC, Shaffer RW, Kincaid CM, Varnier JA, Cheresh DA. Definition of two angiogenic pathways by distinct α_v integrins. *Science* 1995;270:1500–1502. [PubMed: 7491498]
13. Erdreich-Epstein A, Shimada H, Groshen S, Liu M, Metelitsa LS, Kim KS, Stins MF, Seeger RC, Durden DL. Integrins $\alpha_v\beta_3$ and $\alpha_v\beta_5$ are expressed by endothelium of high-risk neuroblastoma and their inhibition is associated with increased endogenous ceramide. *Cancer Res* 2000;60:712–721. [PubMed: 10676658]
14. Pasqualini R, Koivunen E, Kain R, Lahdenranta J, Sakamoto M, Stryhn A, Ashmun RA, Shapiro LH, Arap W, Ruoslahti E. Aminopeptidase N is a receptor for tumor-homing peptides and a target for inhibiting angiogenesis. *Cancer Res* 2000;60:722–727. [PubMed: 10676659]
15. Hood JD, Cheresh DA. Role of integrins in cell invasion and migration. *Nat Rev Cancer* 2002;2:91–100. [PubMed: 12635172]
16. Hynes RO. Integrins: bidirectional, allosteric signaling machines. *Cell* 2002;110:673–687. [PubMed: 12297042]
17. Ruoslahti E. Specialization of tumour vasculature. *Nat Rev Cancer* 2002;2:83–90. [PubMed: 12635171]
18. Arap W, Pasqualini R, Ruoslahti E. Cancer treatment by targeted drug delivery to tumor vasculature in a mouse model. *Science* 1998;279:377–380. [PubMed: 9430587]
19. Healy JM, Murayama O, Maeda T, Yoshino K, Sekiguchi K, Kikuchi M. Peptide ligands for integrin $\alpha_v\beta_3$ Selected from random phage display libraries. *Biochemistry* 1995;34:3948–3955. [PubMed: 7535098]
20. Hart SL, Knight AM, Harbottle RP, Mistry A, Hunger HD, Cutler DF, Williamson R, Coutelle C. Cell binding and internalization by filamentous phage displaying a cyclic Arg-Gly-Asp-containing peptide. *J Biol Chem* 1994;269:12468–12474. [PubMed: 8175653]
21. Aumailley M, Gurrath M, Mueller G, Calvete J, Timpl R, Kessler H. Arg-Gly-Asp constrained within cyclic pentapeptides. Strong and selective inhibitors of cell adhesion to vitronectin and laminin fragment P1. *FEBS Lett* 1991;291:50–54. [PubMed: 1718779]
22. Frisch SM, Francis H. Disruption of epithelial cell-matrix interactions induces apoptosis. *J Cell Biol* 1994;124:619–626. [PubMed: 8106557]
23. Temming K, Schiffelers RM, Molema G, Kok RJ. RGD-based strategies for selective delivery of therapeutics and imaging agents to the tumour vasculature. *Drug Resist Update* 2005;8:381–402.

24. Barnes KR, Kutikov A, Lippard SJ. Synthesis, characterization, and cytotoxicity of a series of estrogen-tethered platinum(IV) complexes. *Chem Biol* 2004;11:557–564. [PubMed: 15123250]
25. Colombo G, Curnis F, De Mori GMS, Gasparri A, Longoni C, Sacchi A, Longhi R, Corti A. Structure-activity relationships of linear and cyclic peptides containing the NGR tumor-homing motif. *J Biol Chem* 2002;277:47891–47897. [PubMed: 12372830]
26. Koivunen E, Wang B, Ruoslahti E. Phage libraries displaying cyclic peptides with different ring sizes: ligand specificities of the RGD-directed integrins. *Bio/Technology* 1995;13:265–270. [PubMed: 9634769]
27. Haubner R, Gratiás R, Diefenbach B, Goodman SL, Jonczyk A, Kessler H. Structural and functional aspects of RGD-containing cyclic pentapeptides as highly potent and selective integrin $\alpha_v\beta_3$ antagonists. *J Am Chem Soc* 1996;118:7461–7472.
28. Boturny D, Coll JL, Garanger E, Favrot MC, Dumy P. Template Assembled Cyclopeptides as Multimeric System for Integrin Targeting and Endocytosis. *J Am Chem Soc* 2004;126:5730–5739. [PubMed: 15125666]
29. The following abbreviations are used throughout this paper: A (Ala), a. A., aminopeptidase-N; BCE, bovine capillary endothelial; bFGF, basic fibroblast growth factor; C (Cys), cysteine; D (Asp), aspartic acid; DIC, 1,3-diisopropylcarbodiimide; DIPEA, diisopropylethylamine; DMEM, Dulbecco's modified Eagle's medium; EDC, 1-[3-(dimethylamino)propyl]-3-ethylcarbodiimide; f, D-phenylalanine; FCS, fetal calf serum; G (Gly), glycine; HMVEC, human microvascular endothelial cell; HOBt, 1-Hydroxybenzotriazole ($C_6H_5N_3O$); IC_{50} , the concentration at which 50% of cell death occurs; L (Leu), leucine; N (Asn), asparagine; NHS, N-hydroxysuccinimide; NMP, N-methyl-2-pyrrolidinone; S (Ser), serine; R (Arg), arginine; TFA, trifluoroacetic acid; TIPS, triisopropylsilane.
30. Dhara SC. A rapid method for the synthesis of *cis*-[Pt(NH₃)₂Cl₂]. *Indian J Chem* 1970;8:193–194.
31. Giandomenico CM, Abrams MJ, Murrer BA, Vollano JF, Rheinheimer MI, Wyer SB, Bossard GE, Higgins JD. Carboxylation of kinetically inert platinum(IV) hydroxy complexes. An entrée into orally active platinum(IV) antitumor agents. *Inorg Chem* 1995;34:1015–1021.
32. Dai X, Su Z, Liu JO. An improved synthesis of a selective $\alpha_v\beta_3$ -integrin antagonist cyclo-(RGDfK-). *Tet Lett* 2000;41:6295–6298.
33. McCusker CF, Kocienski PJ, Boyle FT, Schatzlein AG. Solid-phase synthesis of c(RGDfK) derivatives: on-resin cyclization and lysine functionalization. *Bioorg Med Chem Lett* 2002;12:547–549. [PubMed: 11844669]
34. O'Reilly MS, Holmgren L, Shing Y, Chen C, Rosenthal RA, Moses M, Lane WS, Cao Y, Sage EH, Folkman J. Angiostatin: a novel angiogenesis inhibitor that mediates the suppression of metastases by a Lewis lung carcinoma. *Cell* 1994;79:315–328. [PubMed: 7525077]
35. Short SM, Talbott GA, Juliano RL. Integrin-mediated signaling events in human endothelial cells. *Mol Biol Cell* 1998;9:1969–1980. [PubMed: 9693360]
36. Hambley TW, Battle AR, Deacon GB, Lawrenz ET, Fallon GD, Gatehouse BM, Webster LK, Rainone S. Modifying the properties of platinum(IV) complexes in order to increase biological effectiveness. *J Inorg Biochem* 1999;77:3–12. [PubMed: 10626347]
37. Oh WK, Tay MH, Huang J. Is there a role for platinum chemotherapy in the treatment of patients with hormone-refractory prostate cancer? *Cancer* 2007;109:477–486. [PubMed: 17186531]
38. Carr JL, Tingle MD, McKeage MJ. Rapid biotransformation of satraplatin by human red blood cells in vitro. *Cancer Chemother Pharmacol* 2002;50:9–15. [PubMed: 12111106]
39. Silverman AP, Bu W, Cohen SM, Lippard SJ. 2.4-Å Crystal structure of the asymmetric platinum complex {Pt(amine)(cyclohexylamine)}²⁺ bound to a dodecamer DNA duplex. *J Biol Chem* 2002;277:49743–49749. [PubMed: 12377787]
40. Choi S, Filotto C, Bisanzo M, Delaney S, Lagasee D, Whitworth JL, Jusko A, Li C, Wood NA, Willingham J, Schwenker A, Spaulding K. Reduction and anticancer activity of platinum(IV) complexes. *Inorg Chem* 1998;37:2500–2504.
41. Lemma K, Sargeson AM, Elding LI. Kinetics and mechanism for reduction of oral anticancer platinum (IV) dicarboxylate compounds by L-ascorbate ions. *J Chem Soc Dalton Trans* 2000:1167–1172.

42. Lemma K, Shi T, Elding LI. Kinetics and mechanism for reduction of the anticancer prodrug *trans,trans,trans*-[PtCl₂(OH)₂(c-C₆H₁₁NH₂)(NH₃)] (JM335) by thiols. *Inorg Chem* 2000;39:1728–1734. [PubMed: 12526561]
43. Aida K, Onda M, Asano G, Nakazawa N. Predisposition of subclones of pancreatic carcinoma cells, AsPC-1, to changes in functional and histopathological features of xenograft tumors with response to extracellular matrix. *Nippon Ika Daigaku Zasshi* 1997;64:163–171. [PubMed: 9128054]
44. Arai S, Masumoto A, Otsuki M. Beta1 integrins play an essential role in adhesion and invasion of pancreatic carcinoma cells. *Pancreas* 2000;20:129–137. [PubMed: 10707927]
45. Hong SY, Lee H, You WK, Chung KH, Kim DS, Song K. The snake venom disintegrin salmosin induces apoptosis by disassembly of focal adhesions in bovine capillary endothelial cells. *Biochem Biophys Res Commun* 2003;302:502–508. [PubMed: 12615062]
46. Liu ZJ, Snyder R, Soma A, Shirakawa T, Ziober BL, Fairman RM, Herlyn M, Velazquez OC. VEGF-A and $\alpha_v\beta_3$ integrin synergistically rescue angiogenesis via N-Ras and PI3-K signaling in human microvascular endothelial cells. *FASEB J* 2003;17:1931–1933. [PubMed: 14519669]
47. Yokoyama Y, Ramakrishnan S. Addition of an aminopeptidase N-binding sequence to human endostatin improves inhibition of ovarian carcinoma growth. *Cancer* 2005;104:321–331. [PubMed: 15952188]
48. Stupack DG, Cheresh DA. Integrins and angiogenesis. *Curr Top Dev Biol* 2004;64:207–238. [PubMed: 15563949]
49. Haubner R, Finsinger D, Kessler H. Stereoisomeric peptide libraries and peptidomimetics for designing selective inhibitors of the $\alpha_v\beta_3$ integrin for a new cancer therapy. *Angew Chem Int Ed Engl* 1997;36:1374–1389.
50. Chaleix V, Sol V, Huang YM, Guilloton M, Granet R, Blais JC, Krausz P. RGD-porphyrin conjugates: Synthesis and potential application in photodynamic therapy. *Eur J Org Chem* 2003:1486–1493.
51. Safaei R. Role of copper transporters in the uptake and efflux of platinum containing drugs. *Cancer Lett* 2006;234:34–39. [PubMed: 16297532]
52. Zhang S, Lovejoy K, Shima JE, Lagpacan LL, Shu Y, Lapuk A, Chen Y, Komori T, Gray JW, Chen X, Lippard SJ, Giacomini KM. Organic cation transporters are determinants of oxaliplatin cytotoxicity. *Cancer Res* 2006;66:8847–8857. [PubMed: 16951202]

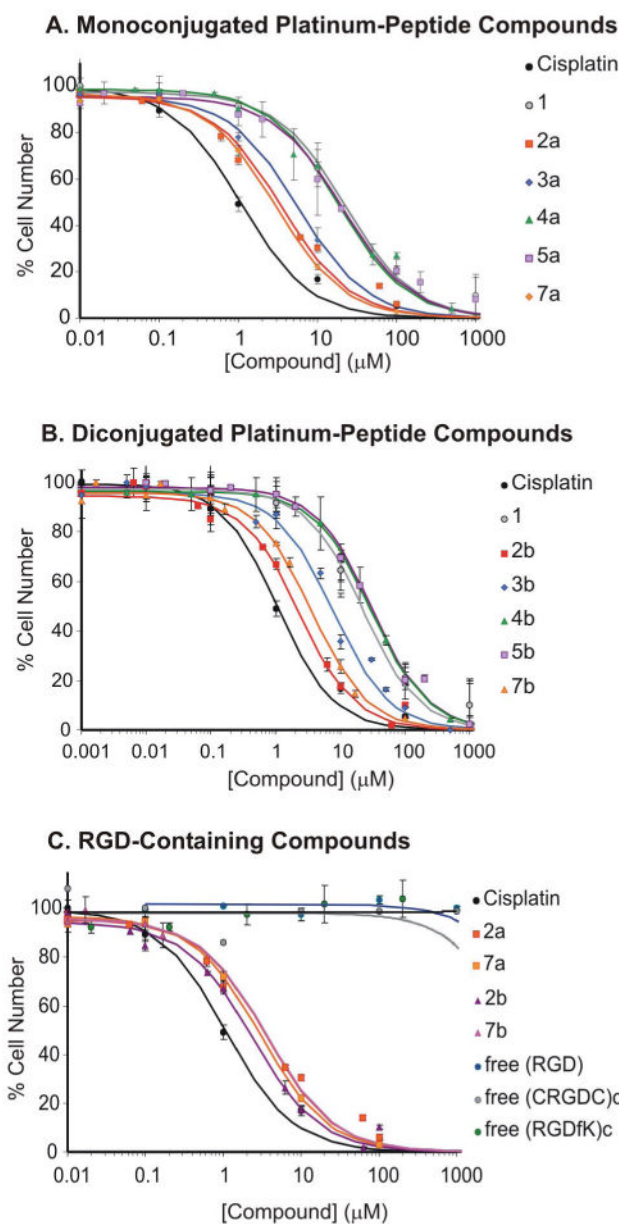


Figure 1. Concentration-response curves of the platinum complexes on BCE cells. (A) Monofunctionalized platinum(IV) complexes along with cisplatin, and 1. (B) Difunctionalized platinum(IV) complexes along with cisplatin, and 1. (C) Pt-RGD complexes and the RGD-containing tri- and pentapeptides. The cells were treated for 72 h with each complex and counted by using a Coulter Counter.

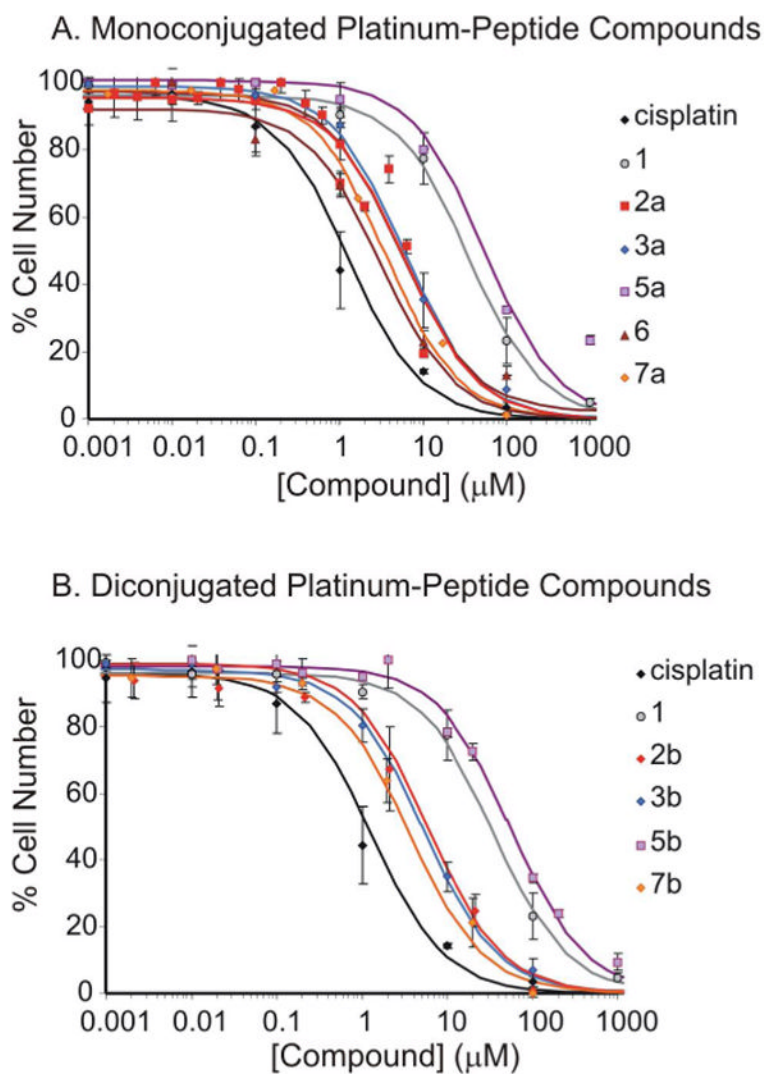


Figure 2. Concentration-response curves of platinum complexes on HMVEC cells. (A) Monofunctionalized platinum(IV) complexes along with cisplatin and **1**. (B) Difunctionalized platinum(IV) complexes along with cisplatin, and **1**. The cells were treated for 72 h with each complex and counted using Coulter counter.

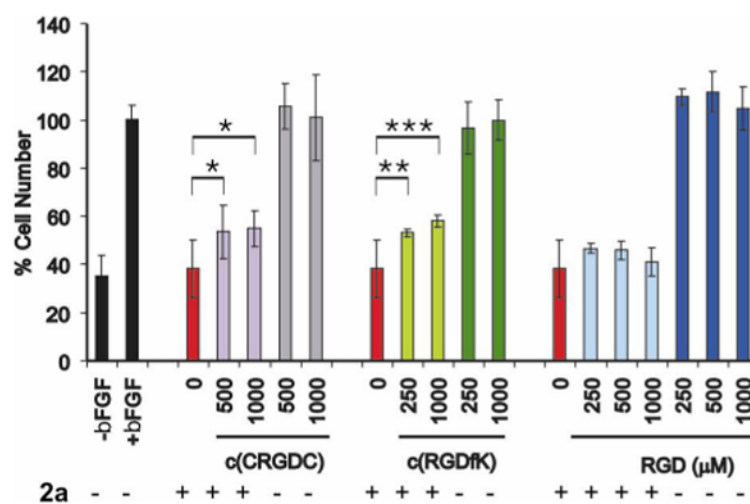


Figure 3. Competition of 2a with RGD peptides in BCE cells

bFGF-stimulated BCE cells treated with **2a** (2 μ M) either alone (red) or in the presence of a large excess of RGD-containing peptides: (CRGDC)c (purple), (RGDfK)c (light green), RGD (light blue). Controls: BCE proliferation with and without bFGF (black), and with bFGF and free RGD-peptides ((CRGDC)c in gray, (RGDfK)c in dark green, and RGD in dark blue). Asterisks indicate statistical significance, as measured with One-way Analysis of Variance (ANOVA), using the Tukey-Kramer multiple comparison test ($P < 0.05$ (*), $P < 0.01$ (**); $P < 0.001$ (***)). Samples run in triplicate; experiments performed in duplicate.

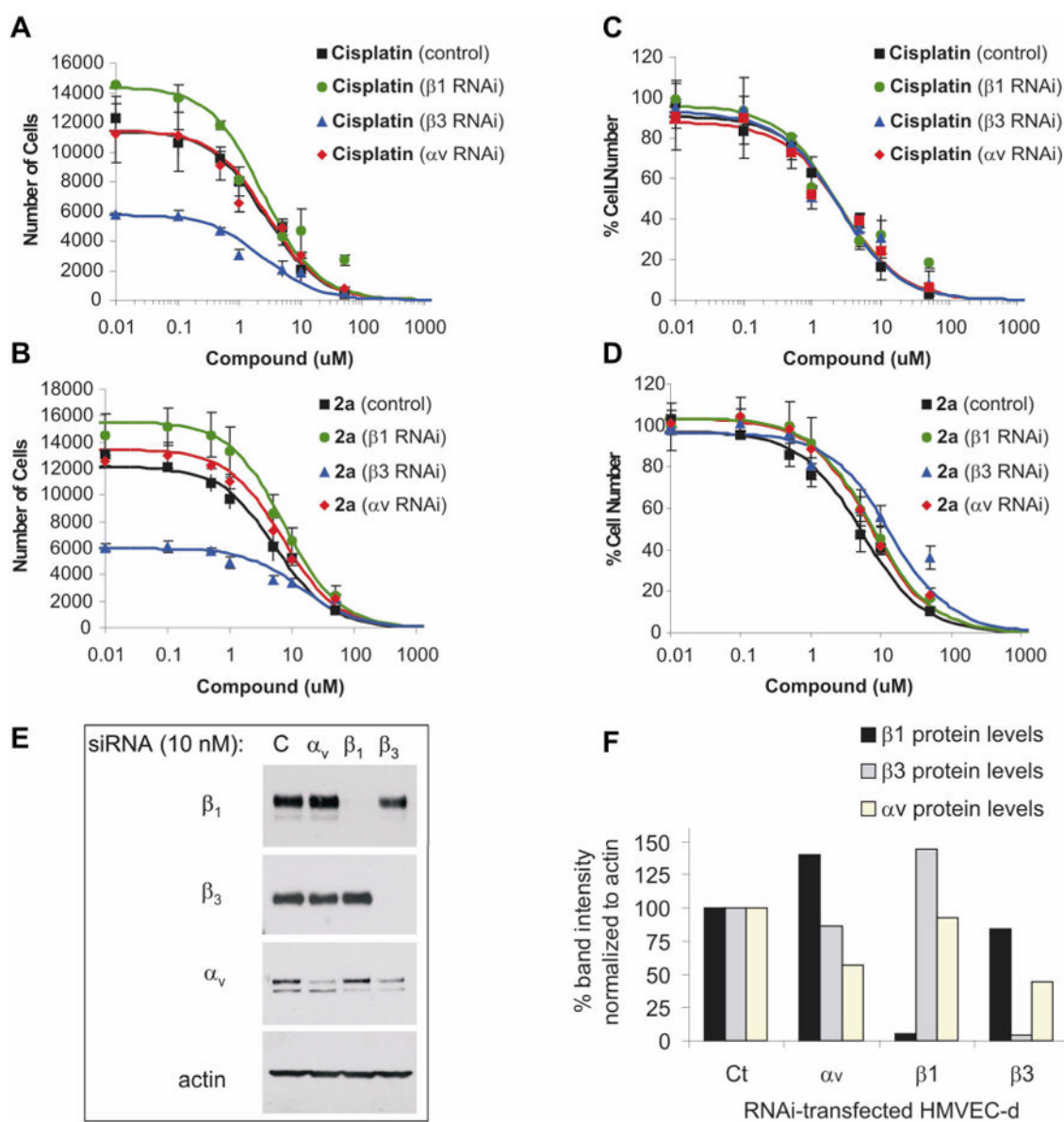


Figure 4. Integrin beta-3 partially mediates Pt(IV)-RGD inhibition of proliferation in HMVEC-d cells

Concentration-response curves in HMVEC-d cells after RNAi knockdown of integrins β_1 , β_3 , or α_v displayed as total cell number (A, B) or percent cell number (C, D) 72 hours after treatment. Poor cell growth was observed in HMVEC-d cells lacking integrin β_3 , but not α_v or β_1 (A, B). Despite differences in cell growth between control, β_1 and β_3 knockdown cells, identical concentration response curves were obtained with cisplatin (C). In contrast, a shift in IC-50 was obtained with **2a** (D), particularly with β_3 knockdown. (E) Western Blot of lysates from transfected HMVEC 120h post-transfection. In lanes: control, α_v , β_1 , and β_3 RNAi transfected HMVEC; in rows: lysates probed with mAb against integrins β_1 , β_3 , α_v , and actin. (F) Gel quantitation and normalization to actin, demonstrating nearly complete knockdown of β_1 and β_3 , increased β_1 levels in α_v -transfected cells, and increased β_3 levels in β_1 -transfected cells. Integrin α_v was significantly decreased (>45%) in both α_v - and β_3 -transfected cells.

Chart 1
Designations, Abbreviations and Charges on Complexes

No.	Complex	Charge at pH 7.0
1	Cisplatin [Pt-(NH ₃) ₂ Cl ₂ (succinate) ₂]	0 -2
2a	Pt-RGD-mono	-1
2b	Pt-RGD-bis	0
3a	Pt-NGR-mono	0
3b	Pt-NGR-bis	+2
4a	Pt-AGR-mono	0
4b	Pt-AGR-bis	+2
5a	Pt-Gly mono	-1
5b	Pt-Gly -bis	0
6	Pt-(CRGDC)c-mono	-1
7a	Pt-(RGDFK)c-mono	-1
7b	Pt-(RGDFK)c-bis	0

Table 1
Expression Level of $\alpha_v\beta_3$ and $\alpha_v\beta_5$ Integrins in Different Cell Lines

Cell Line	% Labeling		
	$\alpha_v\beta_3$	$\alpha_v\beta_5$	APN
BCE	77±12	44±23	25±5
HMVEC	45±3	98±5	96±1
HUVEC	90±5	96±5	n. d.
U87	82±7	94±7	n. d.
ASPC1	12±6	46±5	n. d.
MES-SA	1±1	59±26	n. d.
HeLa	1±0.02	83±13	n. d.

Table 2
IC₅₀ (μM) Values of Platinum Complexes for BCE and HMVEC Cells

Complex	BCE IC ₅₀	P-value	HMVEC IC ₅₀	P-value
Cisplatin	1.1±0.11	****	1.2±0.22	****
1	21±3.0	****	33±3.7	****
2a	3.1±0.33	****	5.5±0.74	****
2b	2.1±0.31	****	4.5±1.4	**
3a	5.1±0.61	****	5.9±0.66	****
3b	7.1±0.86	****	5.1±0.45	****
4a	18±2.2	****	n.d.	
4b	28±3.9	****	n.d.	
5a	19±2.6	****	55±11	***
5b	30±3.4	****	55±6.0	****
6	n.d.		2.7±0.60	**
7a	2.8±0.43	****	3.4±0.67	***
7b	3.4±0.55	****	3.3±0.85	**
2a/cisplatin	2.8		4.5	
7a/cisplatin	2.5		2.8	
5a/cisplatin	17		45	

P-value = P<0.01 (**), P<0.001(***), and P<0.0001 (****).

n.d. = not determined.

Table 3

IC ₅₀ on HMVEC-d	Cisplatin (μM)	P-value	2a (μM)	P-value
Control RNAi	2.2±0.4	**	5.1±0.8	**
Alpha-v RNAi	2.2±0.6	*	7.5±0.7	****
Beta-1 RNAi	2.2±0.8	*	8.0±0.7	***
Beta-3 RNAi	2.2±0.7	*	13 ± 4.3	*

P-value = P<0.05 (*), P<0.01 (**), P<0.001(***), and P<0.0001 (****).

n.d. = not determined.

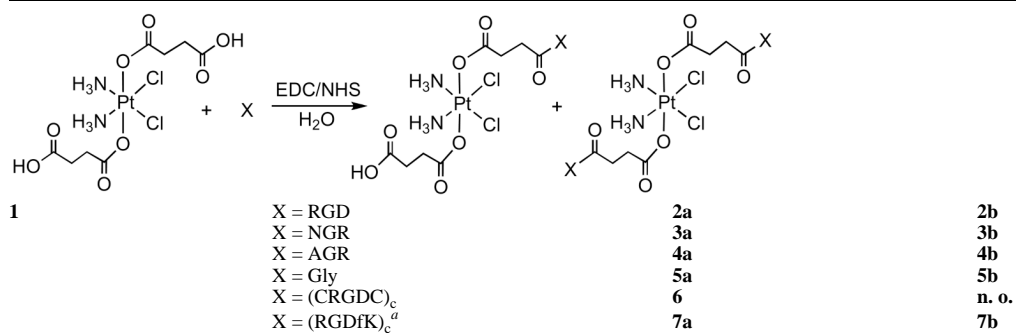
Table 4
Inhibition by Cisplatin and RGD-Targeted Pt(IV) Compounds in Endothelial and Non-Endothelial Cells

IC ₅₀ /Cell	HUVEC	U87	ASPC1	MES-SA	HeLa
Cisplatin	0.52±0.08 ****	0.38±0.09 ****	0.24±0.08 **	0.15±0.03 ****	1.3±0.22 ****
2a	2.6±0.31 ****	1.6±0.61 *	0.79±0.19 **	1.7±0.33 ***	4.6±0.79 ****
2b	11±2.8 **	3.6±0.66 ****	1.5±0.38 **	1.3±0.19 ****	3.5±0.96 **
6	4.2±0.6 ****	1.5±0.58 *	n. d.	3.9±1.1 **	n. d.
7a	3.5±0.51 ****	0.99±0.10 ****	1.6±0.51 *	0.59±0.12 ****	3.9±0.81 **
7b	5.9±1.2 ****	0.66±0.15 **	2.1±0.62 *	0.41±0.05 ****	4.9±0.85 *
5a	110±29 **	20±7 *	n. d.	13±3.2 **	n. d.
5b	45±14 **	50±9.7 ****	n. d.	6.8±1.3 ***	n. d.
2a/cisplatin	5.0	4.2	3.3	11	3.5
7a/cisplatin	6.7	2.6	6.6	3.9	3.0
5a/cisplatin	211	52	n. d.	87	n. d.

P-value = P<0.05 (*), P<0.01 (**), P<0.001 (***), and P<0.0001 (****).

n. d. = not determined.

Scheme 1
Synthesis and Labeling of Complexes



n. o. = not observed

* ε-amino group of the lysine side chain was activated by using a base, DIPEA, before reacting it with **1**.